

Search for leptonic decays of the dark photon at NA62The NA62 collaboration¹¹*Full author list given at the end of the Letter.*
(Dated: 18 December 2023)

The NA62 experiment at CERN, configured in beam-dump mode, has searched for dark photon decays in flight to electron-positron pairs using a sample of 1.4×10^{17} protons on dump collected in 2021. No evidence for a dark photon signal is observed. The combined result for dark photon searches in lepton-antilepton final states is presented and a region of the parameter space is excluded at 90% CL, improving on previous experimental limits for dark photon mass values between 50 and 600 MeV/ c^2 and coupling values in the range 10^{-6} to 4×10^{-5} . An interpretation of the e^+e^- search result in terms of the emission and decay of an axion-like particle is also presented.

I. INTRODUCTION

The prevalence of dark matter over ordinary matter, one of the unsolved puzzles of the universe, has inspired various extensions of the Standard Model (SM). Some of these predict the existence of an additional $U(1)$ gauge-symmetry sector with a vector mediator field A' known as the “dark photon”.

Minimalistic dark photon models [1, 2] introduce the A' field with mass $M_{A'}$, which interacts with the gauge field B associated with the SM $U(1)$ symmetry through kinetic mixing, with its strength characterised by the coupling constant ε . The dark photon may also interact with additional fields in the dark sector. Under the assumption that $M_{A'}$ is lower than twice the mass of the lightest state in the dark sector, the dark photon decays to SM particles only. Cosmological constraints on the thermal relic density of dark matter favour a dark photon mass range from 1 to 1000 MeV/ c^2 , together with ε within the range 10^{-6} to 10^{-3} [3–5].

The search for a dark photon decaying into e^+e^- is described here. The result of this search in combination with a previous result [6] for the $A' \rightarrow \mu^+\mu^-$ decay is presented. A scenario of emission of an axion-like particle (ALP) coupled to the SM fermionic fields is also considered.

II. BEAMLINER AND DETECTOR

Figure 1 illustrates the NA62 beamline and detector layout. A comprehensive description of these components can be found in [7]. In standard operation, kaons are produced by 400 GeV/ c protons extracted from the CERN SPS impinging on a beryllium target. In dump-mode operation, the beryllium target is removed, and the

protons interact in a 3.2 m long absorber (TAX) equivalent to 19.6 nuclear interaction lengths. The origin of the coordinate system is in the centre of the target. The Z axis points in the proton beam direction, the Y axis points upwards, and the X,Y,Z axes form a right-handed system. The mean position of the primary protons at the TAX entrance is (0, -22 mm, 23 m).

The momenta and directions of charged particles within the fiducial volume (FV) are measured by a magnetic spectrometer (STRAW). A quasi-homogeneous liquid krypton electromagnetic calorimeter (LKr) and a muon detector (MUV3) are used for particle identification. Twelve ring-shaped lead-glass detectors (LAV1–12) record activity originating from secondary interactions. Two scintillator hodoscopes, NA48-CHOD and CHOD, provide trigger signals and time measurements for charged particles with 200 ps and 800 ps precision, respectively. The ANTI0 scintillator hodoscope [8] is used to detect charged particles produced upstream of the FV. Further details of the beam-dump mode operation are given in [6].

III. ANALYSIS STRATEGY AND EVENT SELECTION

The search is based on the data sample collected in a 10-day period in 2021, corresponding to 1.4×10^{17} protons on TAX (POT). Three trigger lines were implemented: Q1 required at least one signal in the CHOD, downscaled by a factor of 20; H2 required in-time signals in two CHOD tiles; a control trigger required an LKr energy deposit above 1 GeV.

Two-track final states triggered by the H2 condition are considered. Each track reconstructed by the STRAW must satisfy the following criteria: momentum $p >$

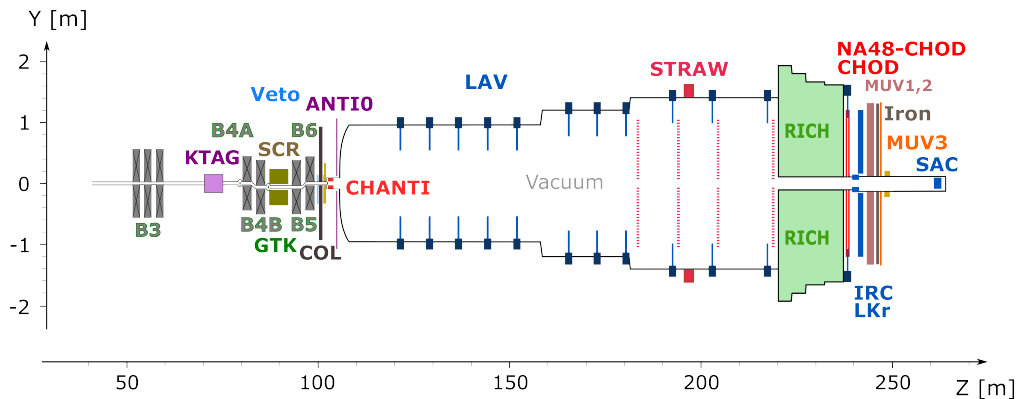


FIG. 1. Schematic side view of the NA62 setup in 2021. Information from KTAG, GTK, CHANTI, MUV1,2, IRC, and SAC is not used in this analysis. Not all beam elements are shown.

10 GeV/c; extrapolated positions at the front planes of NA48-CHOD, CHOD, LKr, MUV3 within the geometrical acceptance of each detector; extrapolated positions at the first STRAW chamber and LKr front planes isolated from those of other tracks. Each track must be associated with a CHOD signal compatible in space and time. The track time is defined using the time of the associated NA48-CHOD signal if present, otherwise using the time of the associated CHOD signal. Track times must be within 5 ns of the trigger time. Tracks spatially compatible and in time with an ANTI0 signal or in time with a LAV signal are rejected.

Any MUV3 signal within a momentum-dependent search radius around the extrapolated track position and within 5 ns of the track time is associated with the STRAW track. An LKr energy deposit $E > 1$ GeV is associated with the track if it is in time and spatially compatible, accounting for possible bremsstrahlung-induced energy deposits. Tracks with an associated MUV3 signal and $E/p < 0.2$ are identified as muons. Tracks without associated MUV3 signals, with $(E/p)_{\min} < E/p < 1.05$ are identified as electrons, where $(E/p)_{\min} = 0.95$ for $p < 150$ GeV/c and decreases with momentum otherwise.

The presence of exactly one two-track vertex is required. The vertex time is evaluated as the mean time of the two tracks. The vertex position is obtained by the backwards extrapolation of the tracks, accounting for the residual magnetic field in the FV. The data distribution of the vertex longitudinal coordinate (Z_{vtx}) and radial position in the transverse plane (ρ_{vtx}) is shown in Figure 2. This distribution is dominated by secondary interactions in LAV1–5 and the vacuum-tank cap. Most reconstructed vertices originate from secondary interactions in LAV5 ($Z \simeq 152$ m). LAV6–12 have larger inner radii (Figure 1) and do not block the resulting particles. It is required that the vertex is reconstructed in the restricted FV, defined as shown in Figure 2, to reject these interactions.

The position of the A' production point is evaluated as the point of closest approach between the A' line of

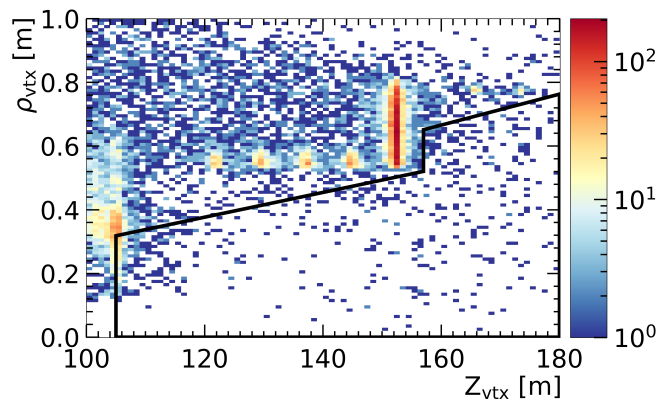


FIG. 2. Distribution of two-track vertex positions in the plane (Z_{vtx} , ρ_{vtx}) for data events, without particle identification requirements. The black contour defines the restricted FV.

flight, defined by the two-track vertex position and total momentum direction, and the beam line, parallel to the Z axis and defined by the average impact point of the primary protons in the TAX. The signal region (SR) is defined as an ellipse in the plane of the Z coordinate (Z_{TAX}) of the A' production point and the distance between the two lines (CDA_{TAX}):

$$\text{SR} : \left(\frac{Z_{\text{TAX}}[\text{m}] - 23}{12} \right)^2 + \left(\frac{\text{CDA}_{\text{TAX}}[\text{m}]}{0.03} \right)^2 < 1. \quad (1)$$

This condition reduces the signal acceptance by 1.7% as shown by simulation. The control region (CR) used to validate the background estimate is the area outside SR that satisfies:

$$\text{CR} : -4 < Z_{\text{TAX}} < 50 \text{ m and } \text{CDA}_{\text{TAX}} < 0.15 \text{ m.} \quad (2)$$

Both SR and CR are kept masked until validation of the background estimate. The data distribution of e^+e^- vertices in the plane (Z_{TAX} , CDA_{TAX}), after applying the

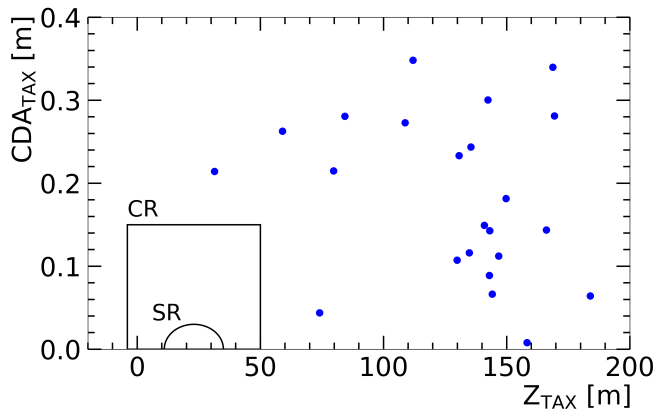


FIG. 3. Data distribution in the plane $(Z_{\text{TAX}}, CDA_{\text{TAX}})$ for e^+e^- vertices without applying the LAV and ANTI0 veto conditions. CR and SR are masked.

full selection except for the LAV and ANTI0 veto conditions, is shown in Figure 3. The full selection removes all events outside SR and CR.

IV. BACKGROUNDS

Mesons produced by proton interactions in the TAX generate a flux of “halo” muons. One source of background consists of vertices in which both particles are created by the same halo muon interacting with the material along the beamline (prompt background). A control data sample is constructed from muons satisfying the Q1 trigger and not the H2 trigger. These muons are extrapolated backwards using PUMAS [9] to the upstream plane of the B5 magnet (Figure 1), and are used as input to a GEANT4-based Monte Carlo (MC) simulation [10]. The resulting events constitute the prompt background sample, which is subjected to the signal selection. The size of this control sample is equivalent to that of the data sample. The expected number of e^+e^- vertices reconstructed in the restricted FV derived from this sample has a relative systematic uncertainty of 50% arising from the limited accuracy of the backward extrapolation and forward propagation.

Another possible source of background is the random pairing of e^+ and e^- tracks originating from different primary proton interactions. This combinatorial background component is evaluated using a data-driven approach, with events triggered by the Q1 condition. Single tracks are paired within a 10 ns time window, building pseudo-events. For each event, the vertex is reconstructed as in the signal selection, and the event is assigned a weight that accounts for the time window and the downscaling factor of the Q1 trigger. This background is found to be an order of magnitude smaller than the prompt background, and is therefore neglected.

The expected numbers of background events in CR and SR are calculated using a combination of frequen-

tist and Bayesian techniques. The rejection factors of the LAV and ANTI0 veto conditions and the CR and SR selection requirements are defined as the proportion of e^+e^- vertices discarded by the corresponding conditions. The posterior probability distribution of each rejection factor is computed from the prompt background sample, assuming a uniform prior and a beta function likelihood. Pseudo-experiments are generated, sampling independently the number of events in the FV and the rejection factors. The expected numbers of background events are

$$N_{\text{bkg}}^{\text{CR}} = 9.7_{-7.3}^{+21.3} \times 10^{-3}, \quad N_{\text{bkg}}^{\text{SR}} = 9.4_{-7.2}^{+20.6} \times 10^{-3} \quad (3)$$

where the uncertainties are quoted at 68% confidence level (CL).

V. STATISTICAL ANALYSIS AND RESULTS

After unmasking the CR, no events are observed, in agreement with the 98.3% probability of observing no counts in the null hypothesis. After unmasking the SR, no events are observed, in agreement with the 98.4% probability of observing no counts in the null hypothesis. The exclusion limits obtained are derived using the CL_s method [11] on a grid of A' mass and coupling values. The test statistic is the profile likelihood ratio [12]:

$$q = -2 \ln \frac{L_{s+b}}{L_b}, \quad (4)$$

computed by maximising separately the numerator and denominator with respect to the nuisance parameters: the number of protons on TAX, the expected number of background events in SR and, for L_{s+b} , the expected signal yield. The observed and expected exclusion contours, and the expected $\pm 1\sigma$ and $\pm 2\sigma$ bands, in the $(M_{A'}, \epsilon)$ plane are shown in Figure 4-left.

The combination of this $A' \rightarrow e^+e^-$ result with the NA62 $A' \rightarrow \mu^+\mu^-$ result [6] is performed with the same test statistic but with total likelihoods expressed as products of contributions from the individual A' decay channels. The exclusion regions obtained are shown in Figure 4-right.

The interpretation of this e^+e^- result in terms of the emission of ALPs in $b \rightarrow s$ transition for a set of ALP mass values is shown in Figure 5. A model-independent approach is used, where the ALP lifetime τ_a , its mass M_a and the product $\text{BR}(B \rightarrow K^{(*)}a) \times \text{BR}(a \rightarrow e^+e^-)$ are treated as free parameters. The NA62 limits extend beyond the region excluded by the CHARM experiment [14] in a mass range from 10 to 800 MeV/ c^2 .

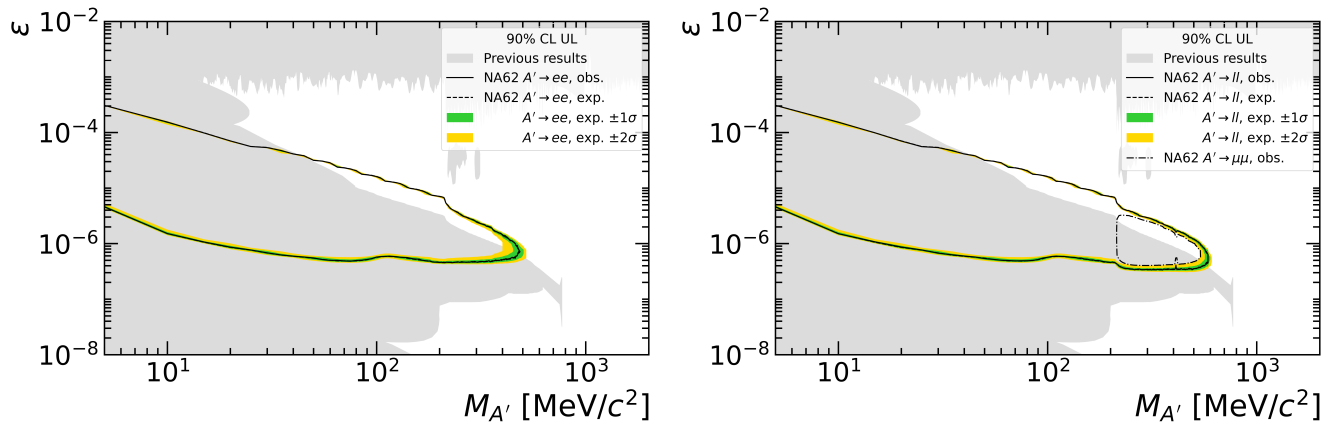


FIG. 4. Observed and expected exclusion contours in the plane $(M_{A'}, \epsilon)$ for the $A' \rightarrow e^+e^-$ analysis (left) and the combined $A' \rightarrow e^+e^-$ and $A' \rightarrow \mu^+\mu^-$ analyses (right) together with the expected $\pm 1\sigma$ (green) and $\pm 2\sigma$ (yellow) bands. Previous results, including the recent FASER result [13] are shown in grey. The NA62 $A' \rightarrow \mu^+\mu^-$ search result [6] is shown with a dot-dashed line in the right panel.

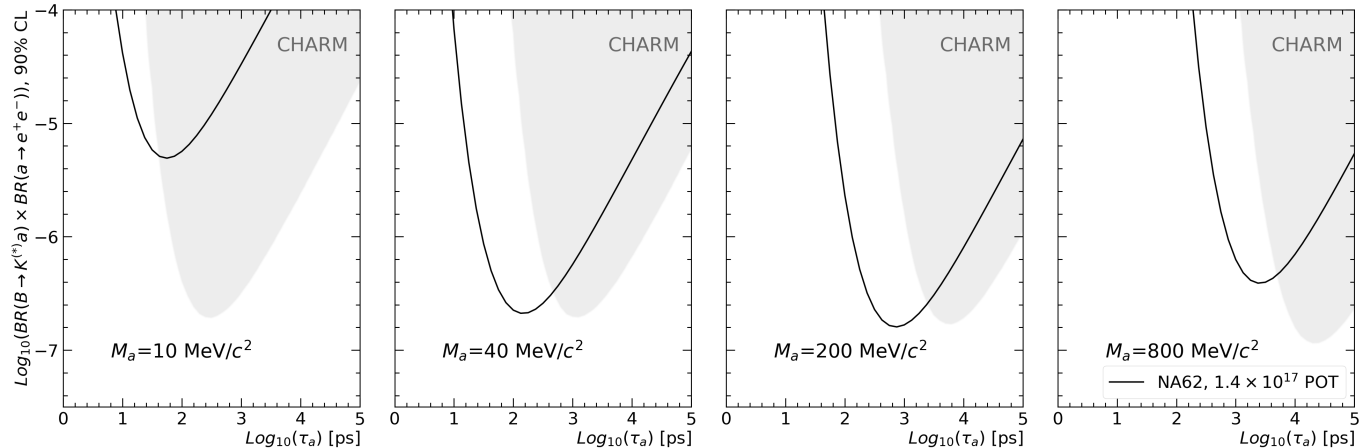


FIG. 5. Exclusion region in the $(\text{ALP lifetime}, \text{BR}(B \rightarrow K^{(*)}a) \times \text{BR}(a \rightarrow e^+e^-))$ plane at 90% CL in the search for an axion-like particle a produced in B meson decays (solid curve). Four mass values are considered. The excluded regions by the CHARM experiment [14] are shown as shaded areas.

VI. CONCLUSION

A search for the decay of a dark photon to the e^+e^- final state utilising data taken in beam-dump mode at the NA62 experiment in 2021 is presented. No event is found in the signal region. A statistical combination with a previous search for the $\mu^+\mu^-$ final state by NA62 is performed, extending the previous exclusion limits on dark photons in the mass range from 50 to 600 MeV/c^2 and coupling constant range 10^{-6} to 4×10^{-5} . This is compatible with thermal relic density constraints. The interpretation of the e^+e^- result in terms of the emission of ALPs coupled to the SM fermionic field is also performed, extending the excluded regions in a mass range from 10 to 800 MeV/c^2 .

ACKNOWLEDGEMENTS

It is a pleasure to express our appreciation to the staff of the CERN laboratory and the technical staff of the participating laboratories and universities for their efforts in the operation of the experiment and data processing.

The cost of the experiment and its auxiliary systems was supported by the funding agencies of the Collaboration Institutes. We are particularly indebted to: F.R.S.-FNRS (Fonds de la Recherche Scientifique - FNRS), under Grants No. 4.4512.10, 1.B.258.20, Belgium; CECI (Consortium des Equipements de Calcul Intensif), funded by the Fonds de la Recherche Scientifique de Belgique (F.R.S.-FNRS) under Grant No. 2.5020.11 and by the Walloon Region, Belgium; NSERC (Natural Sciences and Engineering Research Council), funding SAPPJ-2018-0017, Canada; MEYS (Ministry of Ed-

ucation, Youth and Sports) funding LM 2018104, Czech Republic; BMBF (Bundesministerium für Bildung und Forschung) contracts 05H12UM5, 05H15UMCNA and 05H18UMCNA, Germany; INFN (Istituto Nazionale di Fisica Nucleare), Italy; MIUR (Ministero dell’Istruzione, dell’Università e della Ricerca), Italy; CONACyT (Consejo Nacional de Ciencia y Tecnología), Mexico; IFA (Institute of Atomic Physics) Romanian CERN-RO Nr. 10/10.03.2020 and Nucleus Programme PN 19 06 01 04, Romania; MESRS (Ministry of Education, Science, Research and Sport), Slovakia; CERN (European Organization for Nuclear Research), Switzerland; STFC (Science and Technology Facilities Council), United Kingdom; NSF (National Science Foundation) Award Numbers 1506088 and 1806430, U.S.A.; ERC (European Re-

search Council) “UniversaLepto” advanced grant 268062, “KaonLepton” starting grant 336581, Europe.

Individuals have received support from: Charles University (Research Center UNCE/SCI/013, grant PRIMUS 23/SCI/025), Czech Republic; Czech Science Foundation (grant 23-06770S); Ministero dell’Istruzione, dell’Università e della Ricerca (MIUR “Futuro in ricerca 2012” grant RBFR12JF2Z, Project GAP), Italy; the Royal Society (grants UF100308, UF0758946), United Kingdom; STFC (Rutherford fellowships ST/J00412X/1, ST/M005798/1), United Kingdom; ERC (grants 268062, 336581 and starting grant 802836 “AxScale”); EU Horizon 2020 (Marie Skłodowska-Curie grants 701386, 754496, 842407, 893101, 101023808).

-
- [1] L. B. Okun, *Sov. Phys. JETP* **56**, 502 (1982).
 - [2] B. Holdom, *Physics Letters B* **166**, 196 (1986).
 - [3] C. Boehm and P. Fayet, *Scalar dark matter candidates*, *Nuclear Physics B* **683**, 219 (2004).
 - [4] M. Pospelov, A. Ritz, and M. Voloshin, *Secluded wimp dark matter*, *Physics Letters B* **662**, 53 (2008).
 - [5] J. L. Feng and J. Kumar, *Dark-matter particles without weak-scale masses or weak interactions*, *Phys. Rev. Lett.* **101**, 231301 (2008).
 - [6] E. Cortina Gil *et al.* (NA62 Collaboration), *Journal of High Energy Physics* **09**, 035 (2023).
 - [7] E. Cortina Gil *et al.* (NA62 Collaboration), *J. of Instrumentation* **12**, P05025 (2017).
 - [8] H. Danielsson *et al.*, *J. of Instrumentation* **15**, C07007 (2020).
 - [9] V. Niess, A. Barnoud, C. Cârloganu, and E. Le Méneúeu, *Computer Physics Communications* **229**, 54 (2018).
 - [10] J. Allison *et al.*, *Nucl. Instrum. Meth. A* **835**, 186 (2016).
 - [11] T. Junk, *Nucl. Instrum. Meth. A* **434**, 435 (1999).
 - [12] G. Cowan, K. Cranmer, E. Gross, and O. Vitells, *Eur. Phys. J. C* **71**, 1554 (2011).
 - [13] FASER Collaboration, (2023), arXiv:2308.05587 [hep-ex].
 - [14] J. Dorenbosch *et al.* (CHARM Collaboration), *Physics Letters B* **166**, 473 (1986).

The NA62 Collaboration


Université Catholique de Louvain, Louvain-La-Neuve, Belgium

E. Cortina Gil , J. Jerhot ¹ , A. Kleimenova ^{*} ² , N. Lurkin , M. Zamkovsky ³ 

TRIUMF, Vancouver, British Columbia, Canada

T. Numao , B. Velghe , V. W. S. Wong 

University of British Columbia, Vancouver, British Columbia, Canada

D. Bryman ⁴ 

Charles University, Prague, Czech Republic

Z. Hives , T. Husek ⁵ , K. Kampf , M. Koval 

Aix Marseille University, CNRS/IN2P3, CPPM, Marseille, France

B. De Martino , M. Perrin-Terrin 


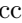

Max-Planck-Institut für Physik (Werner-Heisenberg-Institut), Garching, Germany

B. Döbrich , S. Lezki 


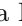


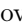
Institut für Physik and PRISMA Cluster of Excellence, Universität Mainz, Mainz, Germany

A. T. Akmete , R. Aliberti ⁶ , L. Di Lella , N. Doble , L. Peruzzo , S. Schuchmann , H. Wahl , R. Wanke 


Dipartimento di Fisica e Scienze della Terra dell'Università e INFN, Sezione di Ferrara, Ferrara, Italy

P. Dalpiaz, I. Neri , F. Petrucci , M. Soldani 

INFN, Sezione di Ferrara, Ferrara, Italy

L. Bandiera , A. Cotta Ramusino , A. Gianoli , M. Romagnoni , A. Sytov 


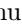
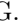




Dipartimento di Fisica e Astronomia dell'Università e INFN, Sezione di Firenze, Sesto Fiorentino, Italy

M. Lenti , P. Lo Chiatto , R. Marchevski ² , I. Panichi , G. Ruggiero 


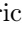







INFN, Sezione di Firenze, Sesto Fiorentino, Italy

A. Bizzeti ⁷ , F. Bucci 

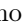
Laboratori Nazionali di Frascati, Frascati, Italy

A. Antonelli , V. Kozhuharov ⁸ , G. Lanfranchi , S. Martellotti , M. Moulson , T. Spadaro , G. Tinti 








Dipartimento di Fisica "Ettore Pancini" e INFN, Sezione di Napoli, Napoli, Italy

F. Ambrosino , M. D'Errico , R. Fiorenza ⁹ , R. Giordano , P. Massarotti , M. Mirra , M. Napolitano , I. Rosa , G. Saracino 

Dipartimento di Fisica e Geologia dell'Università e INFN, Sezione di Perugia, Perugia, Italy

G. Anzivino 

INFN, Sezione di Perugia, Perugia, Italy

F. Brizioli ³ , P. Cenci , V. Duk , R. Lollini , P. Lubrano , M. Pepe , M. Piccini 

Dipartimento di Fisica dell'Università e INFN, Sezione di Pisa, Pisa, Italy

F. Costantini¹, M. Giorgi¹, S. Giudici¹, G. Lamanna¹, E. Lari¹, E. Pedreschi¹, J. Pinzino¹, M. Sozzi¹

INFN, Sezione di Pisa, Pisa, Italy

R. Fantechi¹, F. Spinella¹

Scuola Normale Superiore e INFN, Sezione di Pisa, Pisa, Italy

I. Mannelli¹

Dipartimento di Fisica, Sapienza Università di Roma e INFN, Sezione di Roma I, Roma, Italy

M. Raggi¹

INFN, Sezione di Roma I, Roma, Italy

A. Biagioni¹, P. Cretaro¹, O. Frezza¹, A. Lonardo¹, M. Turisini¹, P. Vicini¹

INFN, Sezione di Roma Tor Vergata, Roma, Italy

R. Ammendola¹, V. Bonaiuto¹⁰, A. Fucci¹, A. Salamon¹, F. Sargeni¹¹

Dipartimento di Fisica dell'Università e INFN, Sezione di Torino, Torino, Italy

R. Arcidiacono¹², B. Bloch-Devaux¹, E. Menichetti¹, E. Migliore¹

INFN, Sezione di Torino, Torino, Italy

C. Biino¹, A. Filippi¹, F. Marchetto¹, D. Soldi¹

Instituto de Física, Universidad Autónoma de San Luis Potosí, San Luis Potosí, Mexico

A. Briano Olvera¹, J. Engelfried¹, N. Estrada-Tristan¹³, R. Piandani¹, M. A. Reyes Santos¹³, K. A. Rodriguez Rivera¹

Horia Hulubei National Institute for R&D in Physics and Nuclear Engineering, Bucharest-Magurele, Romania

P. Boboc¹, A. M. Bragadireanu, S. A. Ghinescu^{*}, O. E. Hutanu

Faculty of Mathematics, Physics and Informatics, Comenius University, Bratislava, Slovakia

T. Blazek¹, V. Cerny¹, Z. Kucerova³, R. Volpe¹⁴

CERN, European Organization for Nuclear Research, Geneva, Switzerland

J. Bernhard¹, L. Bician¹⁵, M. Boretto¹, A. Ceccucci¹, M. Ceoletta¹, M. Corvino¹, H. Danielsson¹, F. Duval, L. Federici¹, E. Gamberini¹, R. Guida, E. B. Holzer¹, B. Jenninger, G. Lehmann Miotto¹, P. Lichard¹, K. Massri¹, E. Minucci¹⁶, M. Noy, V. Ryjov, J. Swallow¹⁷

School of Physics and Astronomy, University of Birmingham, Birmingham, United Kingdom

J. R. Fry¹, F. Gonnella¹, E. Goudzovski¹, J. Henshaw¹, C. Kenworthy¹, C. Lazzeroni¹, C. Parkinson¹, A. Romano¹, J. Sanders¹, A. Sergi¹⁸, A. Shaikhiev¹⁹, A. Tomczak¹

School of Physics, University of Bristol, Bristol, United Kingdom

H. Heath¹

School of Physics and Astronomy, University of Glasgow, Glasgow, United Kingdom

D. Britton¹, A. Norton¹, D. Protopopescu¹

Physics Department, University of Lancaster, Lancaster, United Kingdom

J. B. Dainton, L. Gatignon¹, R. W. L. Jones¹

Physics and Astronomy Department, George Mason University, Fairfax, Virginia, USA

P. Cooper, D. Coward²⁰, P. Rubin

Authors affiliated with an Institute or an international laboratory covered by a cooperation agreement with CERN

A. Baeva, D. Baigarashev²¹, D. Emelyanov, T. Enik, V. Falaleev¹⁴, S. Fedotov, K. Gorshanov, E. Gushchin, V. Kekelidze, D. Kereibay, S. Kholodenko²², A. Khotyantsev, A. Korotkova, Y. Kudenko, V. Kurochka, V. Kurshetsov, L. Litov⁸, D. Madigozhin, A. Mefodev, M. Misheva²³, N. Molokanova, V. Obraztsov, A. Okhotnikov, I. Polenkevich, Yu. Potrebenikov, A. Sadovskiy, S. Shkarovskiy, V. Sugonyaev, O. Yushchenko

* Corresponding authors: S. Ghinescu, A. Kleimenova,
email: stefan.ghinescu@cern.ch, alina.kleimenova@cern.ch

¹Present address: Max-Planck-Institut für Physik (Werner-Heisenberg-Institut), D-85748 Garching, Germany

²Present address: Ecole Polytechnique Fédérale Lausanne, CH-1015 Lausanne, Switzerland

³Present address: CERN, European Organization for Nuclear Research, CH-1211 Geneva 23, Switzerland

⁴Also at TRIUMF, Vancouver, British Columbia, V6T 2A3, Canada

⁵Also at School of Physics and Astronomy, University of Birmingham, Birmingham, B15 2TT, UK

⁶Present address: Institut für Kernphysik and Helmholtz Institute Mainz, Universität Mainz, Mainz, D-55099, Germany

⁷Also at Dipartimento di Scienze Fisiche, Informatiche e Matematiche, Università di Modena e Reggio Emilia, I-41125 Modena, Italy

⁸Also at Faculty of Physics, University of Sofia, BG-1164 Sofia, Bulgaria

⁹Present address: Scuola Superiore Meridionale e INFN, Sezione di Napoli, I-80138 Napoli, Italy

¹⁰Also at Department of Industrial Engineering, University of Roma Tor Vergata, I-00173 Roma, Italy

¹¹Also at Department of Electronic Engineering, University of Roma Tor Vergata, I-00173 Roma, Italy

¹²Also at Università degli Studi del Piemonte Orientale, I-13100 Vercelli, Italy

¹³Also at Universidad de Guanajuato, 36000 Guanajuato, Mexico

¹⁴Present address: INFN, Sezione di Perugia, I-06100 Perugia, Italy

¹⁵Present address: Charles University, 116 36 Prague 1, Czech Republic

¹⁶Present address: Syracuse University, Syracuse, NY 13244, USA

¹⁷Present address: Laboratori Nazionali di Frascati, I-00044 Frascati, Italy

¹⁸Present address: Dipartimento di Fisica dell'Università e INFN, Sezione di Genova, I-16146 Genova, Italy

¹⁹Present address: Physics Department, University of Lancaster, Lancaster, LA1 4YB, UK

²⁰Also at SLAC National Accelerator Laboratory, Stanford University, Menlo Park, CA 94025, USA

²¹Also at L. N. Gumilyov Eurasian National University, 010000 Nur-Sultan, Kazakhstan

²²Present address: INFN, Sezione di Pisa, I-56100 Pisa, Italy

²³Present address: Institute of Nuclear Research and Nuclear Energy of Bulgarian Academy of Science (INRNE-BAS), BG-1784 Sofia, Bulgaria